Determination of InP(001) surface reconstructions by STM and infrared spectroscopy of adsorbed hydrogen

L. Li
Department of Physics and Laboratory for Surface Study, University of Wisconsin, Milwaukee, Wisconsin 53201

Q. Fu, C. H. Li, B.-K. Han, and R. F. Hicks*
Chemical Engineering Department, University of California, Los Angeles, California 90095

(Received 14 January 2000)

The atomic structure of the InP(001) reconstructions has been identified by scanning tunneling microscopy and infrared spectroscopy of adsorbed hydrogen. The four phases, in order of decreasing phosphorous coverage, are $c(2\times2)/p(2\times2)$, $\theta_P=2.0$ ML; (2×1), $\theta_P=1.0$ ML; $\sigma(2\times4)$, $\theta_P=0.25$ ML, and $\delta(2\times4)$, $\theta_P=0.125$ ML. The (2×2) consists of phosphorous dimers adsorbed onto a layer of P atoms. Removal of the P adatoms at 300 °C, produces the (2×1), which is terminated with a complete layer of buckled phosphorous dimers. Further annealing at 400 to 500 °C, yields the indium-rich $\sigma(2\times4)$ and $\delta(2\times4)$ reconstructions. The $\sigma(2\times4)$ reconstruction comprises a single phosphorous dimer in the top layer and four indium dimers in the second layer. The $\delta(2\times4)$ differs from the $\sigma(2\times4)$ reconstruction in that one of the P atoms is replaced with an In atom to make an In-P heterodimer. This difference is evident by comparison of the intensities of P-H, In-H, and In-H-In stretching vibrations for the two surfaces.

I. INTRODUCTION

The structure of semiconductor surfaces is of great interest because they mediate the chemical reactions that occur during etching, deposition, and processing of materials into solid-state devices.[1,2] One of the principal methods used to investigate surface structure is scanning tunneling microscopy (STM).[3] This technique yields the local density of states with atomic resolution. However, the features seen in the microscope can be difficult to interpret for compound semiconductors, since the images lack chemical specificity and fold together complex electronic and geometric effects. To overcome these uncertainties, sophisticated total energy calculations are performed.[4–7] This technique works well provided the researcher assumes the correct structure, which requires some a priori knowledge of the possibilities.[6,7]

A sound experimental approach is to combine scanning tunneling microscopy with a chemically specific probe. Among the potential choices, high-resolution vibrational spectroscopy stands out for its ability to discern the chemical bonding at individual adsorption sites on a surface. When a compound semiconductor is dosed with hydrogen atoms at room temperature, all the dangling bonds become saturated with the adsorbate, and the frequencies of the *M*-H stretching vibrations are strongly dependent on the element *M*. For example, on gallium arsenide (001), the frequencies of the As-H, terminal Ga-H and bridging Ga-H-Ga vibrations occur at 2200–1950, 1950–1750, and 1750–1100 cm^{-1}, respectively. This has allowed us to analyze the distribution of surface sites on each GaAs(001) reconstruction and to refine our understanding of their structures.[8,9]

The interest in surface structures of indium phosphide (001) has increased in recent years, because it has been demonstrated that they are not simply replicas of their GaAs(001) counterparts. For example, a (2×1) reconstruction is formed that contains a complete layer of buckled phosphorous dimers.[10,11] This phase is unique to indium phosphide, and has yet to be encountered on other (001) III/V semiconductor surfaces. In addition, at higher phosphorous coverage, one can obtain a (2×2) reconstruction, as observed by reflectance high-energy electron diffraction[12] (RHEED) and recently by STM.[11,13] As for the indium-rich phases, several researchers have examined their structures, but no consensus has emerged as to the arrangement of the indium and phosphorous atoms.[2,14–18] During chemical beam epitaxy of InP, a (2×4) reconstruction has been detected by reflectance difference spectroscopy (RDS) and RHEED.[12,14] It has been argued that the (2×4) reconstruction is composed of phosphorous dimers separated by dimer vacancies, in analogy to GaAs(001). However, Johal *et al.*[15] and Goletti *et al.*[16] studied decapped InP(001) by RDS, and could not explain their spectra using a conventional dimer-vacancy model. MacPherson *et al.* obtained a (2×4) reconstruction by annealing an InP crystal in vacuum.[17] Their filled-state scanning tunneling micrographs revealed that the unit cell contains three bright spots arranged in an equilateral triangle. These authors proposed that the spots were due to the filled dangling bonds of a phosphorous trimer. More recently, several researchers performed total energy calculations on several models of the (2×4) reconstruction, and concluded that the lowest energy phase is a single In-P dimer sitting on a layer of indium.[7,18] The three spots seen in the STM image arise from a filled P dangling bond and two In-In back bonds.

Herein, we report on a study of the InP(001) reconstructions. With the aid of scanning tunneling microscopy and vibrational spectroscopy, the controversies associated with the InP surface structures have been resolved. In particular, we have found that upon heating the crystal, the phosphorous-rich (2×1) reconstruction is transformed sequentially into the indium-rich $\sigma(2\times4)$ and $\delta(2\times4)$

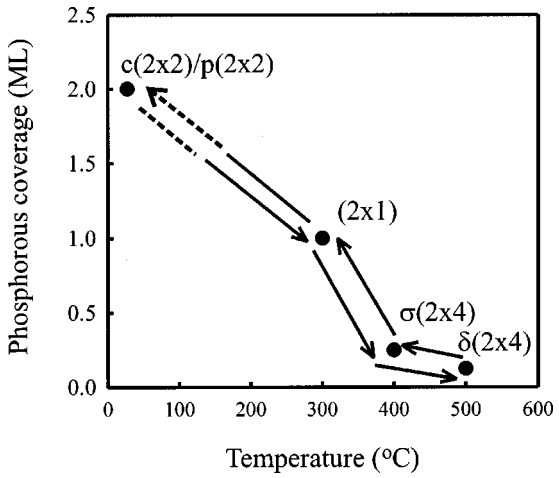

FIG. 1. Surface phases of InP(001) as a function of phosphorus coverage and temperature.

phases. The former reconstruction is terminated with a single phosphorous dimer, while the latter one is terminated with an In-P dimer. Both expose indium dimers in the underlying layer. The surface phase diagram and corresponding reconstructions are described below.

II. EXPERIMENTAL METHODS

Indium phosphide films, 0.5 μm thick, were grown on (001) substrates by metalorganic vapor-phase epitaxy (MOVPE). The following conditions were used during the growth: 600 °C, 20 Torr of hydrogen, 6.5×10^{-4} Torr of triisopropylindium (TIPIn), $(3.2-13.0)\times10^{-2}$ Torr of tertiarybutylphosphine (TBP) (V:III ratio of 50–200), and a total flow rate of 2.5 l/min (at 25 °C and 1 atm). After shutting off the TIPIn supply, TBP and hydrogen flows were maintained until samples were cooled to 300 and 40 °C, respectively. Then the crystals were transferred directly to an ultrahigh vacuum (UHV) chamber without air exposure.

In the UHV chamber, the samples were annealed at temperatures between 100 and 500 °C to obtain the desired reconstructions. After cooling the samples to 25 °C, the surface ordering was characterized by a Princeton Instruments low-energy electron diffractometer (LEED). Scanning tunneling micrographs were recorded with a Park Scientific AutoProbe VP at a tunneling current of 0.5 nA and a sample bias between −3.0 and −4.0 V. Empty-state images were also obtained at a bias of +2.0 to +3.0 V. These images did not reveal any new features, so only the filled states are presented in this paper. Infrared spectra were acquired with a BIO-RAD FTS-40A spectrometer by multiple internal reflection through a trapezoidal crystal, $40.0\times10.0\times0.64\,\mathrm{mm}^3$, with 31 reflections off the front face. The resolution was 8 cm^{-1}. The spectra presented in this paper show the change in reflectance (per reflection) that results from taking the ratio of the sample spectrum at saturation hydrogen coverage to that at zero coverage.

III. RESULTS AND DISCUSSION

Shown in Fig. 1 is the dependence of the surface reconstruction and phosphorous coverage on the annealing temperature in vacuum. Upon transfer from the MOVPE reactor, the semiconductor surface is covered with hydrogen atoms, alkyl groups, and phosphorous ad-dimers.[13] Gentle heating to 150±25 °C removes the hydrogen and organic compounds, and produces a P-rich phase with local $p(2\times2)$ and $c(2\times2)$ domains. The phosphorous coverage at this point is between 1.75 and 1.50 ML. Further heating to 300 °C in vacuum removes the P ad-dimers and generates a (2×1) structure with a coverage of 1.0 ML.[10] Upon annealing the InP crystal at higher temperatures the (2×1) structure is gradually transformed into the $\sigma(2\times4)$ phase. At 400 °C, the $\sigma(2\times4)$ phase comprises most of the surface, yielding a phosphorous coverage close to 0.25 ML. This phase converts into the $\delta(2\times4)$ phase with a phosphorous coverage of 0.125 ML at 500 °C. The phase transformations observed during heating can be reversed by dosing the $\delta(2\times4)$ phase with phosphine at progressively lower temperatures from 400 to 300 °C. The most P-rich reconstruction achievable in vacuum is the (2×1). Nevertheless, exposing the sample to a high flux of the phosphorous precursor in the MOVPE reactor will convert the surface back into the $c(2\times2)/p(2\times2)$ structure.

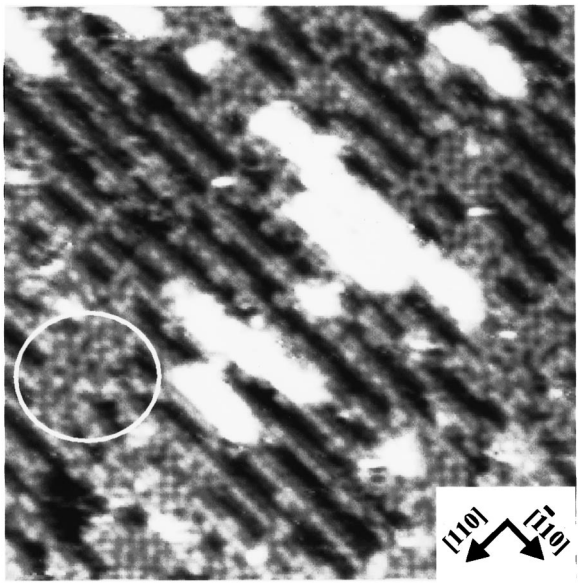

FIG. 2. Scanning tunneling micrograph of the InP(001) surface annealed at 400 °C for 5 min (image size $260\times260\,\text{Å}^2$; sample bias −3.8 V).

In Fig. 2, we present a scanning tunneling micrograph of a mixed $(2\times1)/\sigma(2\times4)$ reconstruction. This image was obtained by annealing the sample for only 5 min at 400 °C. The (2×1) domains are evident as the zigzagging rows of gray spots that extend along the [110] direction. These rows are due to phosphorous dimers that are alternately buckled to the left and to the right. They account for about 40% of the total surface area. A white circle highlights one of the (2×1) regions, in which there is considerable disorder among the dimer rows. This is due to desorption of some of the P atoms. The $\sigma(2\times4)$ structures can be seen as alternating light and dark gray rows that are parallel to the $[\bar{1}10]$ axis. These domains are not well ordered either, and one can discern $\alpha(2\times4)$ unit cells randomly distributed within the $\sigma(2\times4)$ phase.

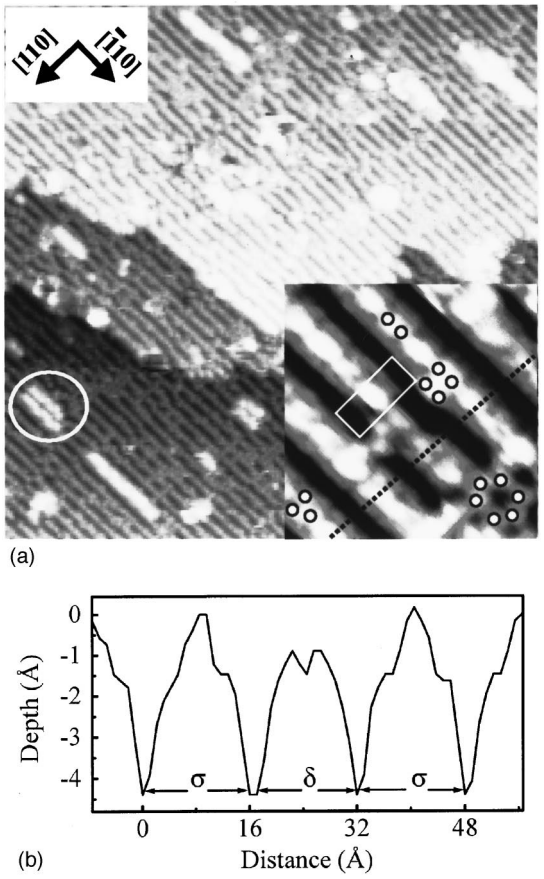

FIG. 3. (a) Scanning tunneling micrograph of the $\sigma(2\times4)$ reconstruction (740×740 Å; inset 65×65 Å; sample bias −3.0 V), and (b) line scan through four unit cells as illustrated by the dotted line in the inset of (a).

Annealing at 400 °C for 20 min in 1.0×10^{-5} Torr of phosphine generates the surface pictured in Fig. 3(a). Here, the characteristic rows of the $\sigma(2\times4)$ phase extend for long distances in the $[\bar{1}10]$ axis. However, these rows, and the step edges that follow alongside them, are not perfectly straight due to many kinks within the rows. In addition, about 10% of the surface is covered with islands, two-atom layers in height, that consist of one or two gray rows, ranging from two to twenty unit-cell widths in the $[\bar{1}10]$ direction. One such island is circled in the image. The two-dimensional (2D) islands appear after repeated cycling between the (2×1), $\sigma(2\times4)$, and $\delta(2\times4)$ reconstructions. Since the $\sigma(2\times4)$ phase has a lower indium coverage than the $\delta(2\times4)$ phase, 0.75 ML In versus 0.875 ML In, some of the indium gets ejected onto the surface and nucleates the small 2D islands.

A close up of the InP(001) surface is shown in the inset in the lower right corner of Fig. 3(a). The white rectangle traces out the dimensions of the (2×4) unit cell. Four different reconstructions can be seen in this image. The dominant reconstruction is the $\sigma(2\times4)$, which consists of two white spots sitting between a gray ledge and a black trench on either side. This structure is highlighted with the two open circles in the top center portion of the picture. Moving down along the same row, another (2×4) cell is encountered that contains four white spots. This is most likely the $\alpha(2\times4)$ reconstruction, which is common on GaAs(001).[3] We have found that on InP(001), this structure is not as stable as the $\sigma(2\times4)$ or $\delta(2\times4)$ phases and never occupies more than a few percent of the surface area. In the lower right corner of the inset, one sees a circle of six highlighted white spots. This pattern is produced by the out-of-phase buckled phosphorous dimers of the remaining (2×1) reconstruction.[10] Small (2×1) domains cover approximately 5% of the total area. Finally, in the lower left corner of the inset, a set of three circles accentuates the trimer feature of the $\delta(2\times4)$, which is discussed below.

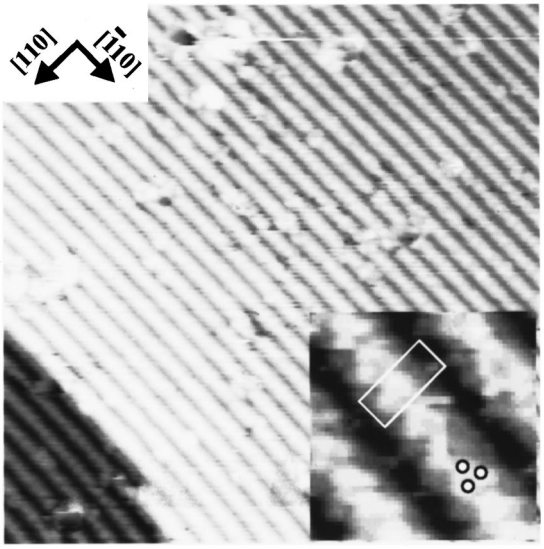

FIG. 4. Scanning tunneling micrograph of the $\delta(2\times4)$ structure (440×440 Å; inset 40×40 Å; sample bias −3.0 V).

A scan of the surface height was taken along the dotted line shown in the inset image, and these results are presented in Fig. 3(b). From left to right, this scan passes over a $\sigma(2\times4)$, a $\delta(2\times4)$, and a $\sigma(2\times4)$ unit cell. For the $\sigma(2\times4)$ phase, the height from the bottom of the trench to the topmost ridge is 4.4 Å, which equals three atomic layers. This distance is consistent with the ridge, i.e., the two white spots, being due to a phosphorous dimer. The height from the bottom of the trench to the intermediate shoulder is 3.1 Å, or a little more than two atomic layers, suggesting that this feature might be due to indium dimers. Now consider the line scan through the $\delta(2\times4)$ unit cell. The height from the bottom of the trench to the top of the two maxima is 3.7 Å, with a local minimum located 0.6 Å below these. The two maxima are located halfway between the shoulder and the top ridge of the $\sigma(2\times4)$ unit cell. These features are not high enough to be associated with phosphorous atoms, as would be the case for a P-trimer structure.[17] Instead, they are more likely due to the indium-indium back-bond states of an In-P heterodimer, as suggested by two recent studies.[7,18]

Annealing the crystal for 20 min at 500 °C produces the most indium-rich reconstruction, the $\delta(2\times4)$ phase. An STM image of this surface is presented in Fig. 4. Uniform gray rows are seen extending along the $[\bar{1}10]$ direction. The surface contains relatively few defects, and the step edges lie straight along the rows. Also note that the two-dimensional islands have disappeared, presumably because the indium content within these islands is consumed in forming the

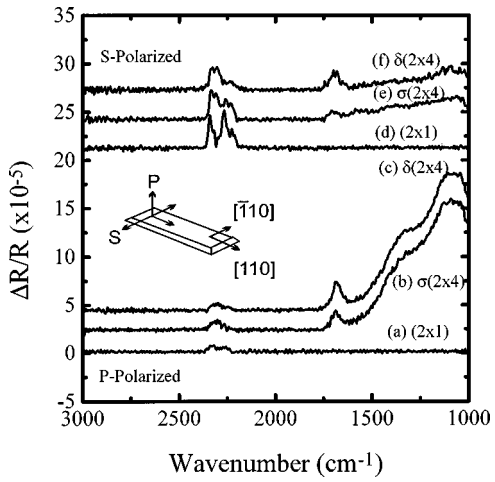

FIG. 5. *s*- and *p*-polarized reflectance spectra of adsorbed hydrogen on the (2×1), $\sigma(2\times4)$, and $\delta(2\times4)$ surfaces at 30 °C.

$\delta(2\times4)$ unit cell. In the inset picture, a closeup of the (2×4) unit cells is shown. Within each cell, one discerns three bright spots in the shape of an equilateral triangle, which has been attributed to an In-P heterodimer.[7,18]

The STM micrographs provide evidence that the $\sigma(2\times4)$ and $\delta(2\times4)$ structures are terminated with a phosphorous dimer and an In-P heterodimer, respectively. In addition, indium dimers may be exposed in the next lower layer. In order to verify these results, the dangling bonds present on these reconstructions have been probed by vibrational spectroscopy of adsorbed hydrogen. Presented in Fig. 5 are the reflectance spectra for saturation coverages of hydrogen on the $\delta(2\times4)$, $\sigma(2\times4)$, and (2×1) reconstructions. The upper three spectra are *s*-polarized, while the lower three spectra are *p*-polarized. According to the inset diagram, the *s*-polarized light probes dipole moments that are parallel to the $[\bar{1}10]$ crystal axis. Inspection of the figure reveals that there are three main sets of bands appearing in the frequency ranges 2350–2200, 1750–1600, and 1600–1000 cm^{-1}. By comparison to the stretching vibrations of known gas-phase molecules, the high-frequency bands may be assigned to phosphorous-hydrogen bonds,[19–21] while the bands in the middle- and low-frequency ranges are most likely due to indium hydrides.[22,23]

In order to assign the vibrational bands to specific bond configurations, *ab initio* calculations have been performed on a series of molecular clusters, including $In_5P_4H_{13}$, $In_4P_5H_{13}$, and $In_7P_8H_{19}$.[24] These clusters are of sufficient size to simulate adsorbed hydrogen on the phosphorous and indium dimers of the (2×1) and (2×4) reconstructions. The structure of the indium phosphide clusters was optimized using density-functional theory.[25] We employed the Perdew-Wang correlation and exchange functional together with the $(18s/14p/9d)/[5s/5p/3d]$ contracted basis set for indium, the Stuttgart-Dresden pseudopotential for phosphorous, and the Dunning-Huzinaga valence double-ζ basis set for hydrogen.[26–30] We have done similar calculations on $Ga_xAs_yH_z$ compounds, and these have provided us with a detailed understanding of the hydrogen adsorption sites on GaAs(001).[31]

In Table I, we present a comparison of the P-H and In-H vibrational modes obtained by experiment and theory. Note

TABLE I. Comparison of the *M*-H vibrational frequencies determined by experiment and theory.

	Frequencies (cm^{-1})	
Assignments	Experiment	Theory
P-H	2339, 2311	2319, 2292
	2213	2190
In-H_t[a]	1660	1504
In-H_b	1350	1138
In-H_b	1150	1195

[a]*t*, terminal; *b*, bridging.

that the predicted In-H stretching frequencies have been shifted down by 220 cm^{-1}. Frequency scaling is employed here to compensate for the systematic error introduced by the computational method.[32] The cluster models reveal that the three P-H stretches are due to phosphorous dihydrogen bonds, and to isolated and coupled phosphorous monohydrogen bonds. The two low-frequency bands at 1350 and 1150 cm^{-1} are assigned to the asymmetric stretch of bridging indium hydride. In the former case, the stretching mode corresponds to an isolated In-H-In structure, while in the latter case, two bridge bonds are coupled together to form an In-H-In-H-In structure. The observation of bridging indium hydride upon adsorption of hydrogen onto the $\sigma(2\times4)$ and $\delta(2\times4)$ reconstructions confirms that indium dimers are present on both of these reconstructions.

Ball-and-stick models for the (2×1), $\sigma(2\times4)$, and $\delta(2\times4)$ structures are given in Fig. 6(a). The (2×1) structure is terminated with a complete layer of phosphorous dimers with each dimer having three electrons in its two dangling bonds.[10] The $\sigma(2\times4)$ structure consists of a single phosphorous dimer straddling four indium dimers, with P and In coverages of 0.25 and 0.75 ML.[18] The $\delta(2\times4)$ structure, on the other hand, differs from the $\sigma(2\times4)$ structure in that the P-P dimer is replaced with an In-P dimer. In this case, the P and In coverages are 0.125 and 0.875 ML. Adsorption of hydrogen atoms onto these reconstructions generates the models in Fig. 6(b). In this case, it is assumed that

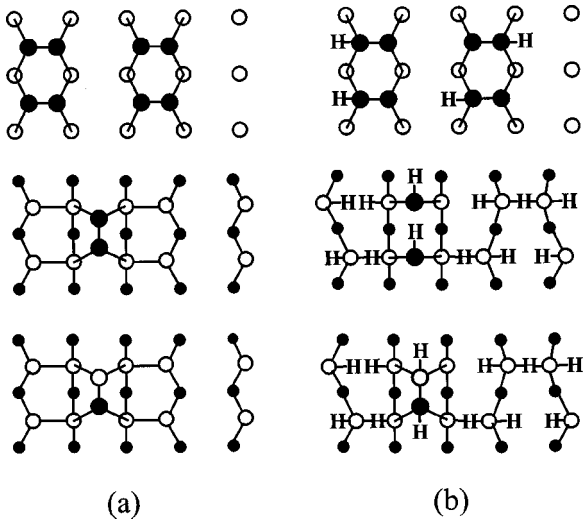

FIG. 6. Ball-and-stick models of the (a) clean and (b) hydrogen-terminated InP(001) reconstructions.

TABLE II. Comparison of the hydrogen coverages to the infrared band intensities.

	Coverage[a]		Intensity[a]	
Structure	θ_{PH}	θ_{InH_b}	I_{PH}	I_{InH_b}
(2×1)	4.0	0.0	3.4	0.0
$\sigma(2\times4)$	2.0	1.0	1.7	0.9
$\delta(2\times4)$	1.0	1.0	1.0	1.0

[a]Normalized to $\delta(2\times4)$.

all the dangling bonds are saturated and the number of electrons involved in bond formation is conserved. The types of structures that can form are more varied than the examples shown but nevertheless illustrate the hydrogen coverages that can be achieved.

The models presented in Fig. 6(b) indicate the relative amounts of adsorbed hydrogen that bonds to phosphorous sites, terminal indium sites, and bridged indium sites. On the (2×1) reconstruction, it is assumed that a hydrogen atom adsorbs on the one-half-filled dangling bond on the phosphorous dimer, yielding a saturation coverage of 0.5 ML. By contrast, on the $\sigma(2\times4)$ and $\delta(2\times4)$ phases, a hydrogen atom may adsorb on each exposed phosphorous atom, leading to saturation coverages of hydrogen on phosphorous sites of 0.25 and 0.125 ML, respectively. Examination of the bridging indium hydrides on each reconstruction gives saturation coverages of hydrogen on these sites of 0.0 ML on the (2×1) structure and 0.375 ML on the $\sigma(2\times4)$ and $\delta(2\times4)$ structures.

For hydrogen adsorption on the same sites, one may assume that the integrated intensities of the *M*-H vibrational bands are proportional to the density of these sites on a given reconstruction. Consequently, a comparison can be made between the relative intensities of these bands and the relative coverages predicted by the models in Fig. 6(b). This comparison is presented in Table II for hydrogen bonded to phosphorous and to indium (bridging In-H-In only). The data have been normalized to the values recorded for the $\delta(2\times4)$ phase. The intensities of the P-H infrared bands on the (2×1) and $\sigma(2\times4)$ phases are 3.4 and 1.7 times greater than that on the $\delta(2\times4)$ phase, which agrees with the coverage ratios of 4.0 and 2.0. Furthermore, the integrated intensity of the bridging indium hydride band is zero on the (2×1) phase and the same value on the $\sigma(2\times4)$ and $\delta(2\times4)$ phases, exactly as predicted by the models. These results provide further evidence that the models of the (2×4) phases in Fig. 6 are correct.

The hydrogen-terminated $\delta(2\times4)$ surface should exhibit a terminal indium hydride bound to an In-P heterodimer. This hydride is unique to this structure, and its dipole moment should extend in a direction that is partly parallel to the $[\bar{1}10]$ direction. Perusal of the *s*-polarized reflectance spectrum for hydrogen adsorbed on the $\delta(2\times4)$ surface reveals a peak for In-H_t at 1683 cm^{-1}, which does not appear in the *s*-polarized spectra of the (2×1) or the $\sigma(2\times4)$ phases. This observation lends additional support for the In-P heterodimer model of the $\delta(2\times4)$ phase.

Two groups have calculated the phase diagram of InP(001) using first-principles pseudopotential calculations.[7,18] These authors predicted the same reconstruction scenario on phosphorous-rich InP(001) as is observed on arsenic-rich GaAs(001), including the formation of $c(4\times4)$, $\beta_2(2\times4)$, and $\alpha(2\times4)$ phases. Under indium-rich conditions, they found that the $\delta(2\times4)$ phase, with the In-P heterodimer, is the most stable reconstruction. In contrast, our experiments reveal that the $c(2\times2)/p(2\times2)$ and (2×1) structures are formed at phosphorous coverages above 1.0 ML, while the $\sigma(2\times4)$ and $\delta(2\times4)$ structures occur below 0.25 ML. Between 1.0 and 0.25 ML, a mixture of (2×1), $\alpha(2\times4)$, $\sigma(2\times4)$, and $\delta(2\times4)$ phases is observed [cf. Fig. 3(a)]. Evidently, the theoretical calculations should be revisited in light of the new experimental data.

IV. SUMMARY

In conclusion, scanning tunneling microscopy used in combination with vibrational spectroscopy of adsorbed hydrogen can provide definitive insight into the composition and structure of compound semiconductor surfaces. With regard to InP(001), we see that the surface phase diagram is not at all like that found on GaAs(001).

ACKNOWLEDGMENTS

Funding for this research was provided by the Office of Naval Research (Grant No. N00014-95-1-0904), and by the National Science Foundation, Division of Materials Research (Grant No. DMR-9804719).

*Corresponding author. Electronic address: rhicks@ucla.edu

[1] J. J. Boland and J. H. Weaver, Phys. Today **51**(8), 34 (1998).
[2] S. D. Adamson, B.-K. Han, and R. F. Hicks, Appl. Phys. Lett. **69**, 3236 (1996).
[3] Q. Xue, T. Hashizume, and T. Sakurai, Prog. Surf. Sci. **56**, 1 (1997).
[4] Q. Xue *et al.*, Phys. Rev. Lett. **74**, 3177 (1995).
[5] L. J. Whitman *et al.*, Phys. Rev. Lett. **79**, 693 (1997).
[6] S. B. Zhang and A. Zunger, Phys. Rev. Lett. **77**, 119 (1996).
[7] S. Mirbt, N. Moll, K. Cho, and J. D. Joannopoulos, Phys. Rev. B **60**, 13 283 (1999).
[8] H. Qi, P. E. Gee, and R. F. Hicks, Phys. Rev. Lett. **72**, 250 (1994).
[9] R. F. Hicks, H. Qi, Q. Fu, B.-K. Han, and L. Li, J. Chem. Phys. **110**, 10 498 (1999).
[10] L. Li, B.-K. Han, Q. Fu, and R. F. Hicks, Phys. Rev. Lett. **82**, 1879 (1999).
[11] P. Vogt, Th. Hannappel, S. Visbeck, K. Knorr, N. Esser, and W. Richter, Phys. Rev. B **60**, R5117 (1999).
[12] K. B. Ozanyan *et al.*, J. Appl. Phys. **82**, 474 (1997).
[13] L. Li, B.-K. Han, D. Law, C. H. Li, Q. Fu, and R. F. Hicks, Appl. Phys. Lett. **75**, 683 (1999).
[14] M. Zorn *et al.*, Appl. Phys. A: Mater. Sci. Process. **65A**, 333 (1997).
[15] T. K. Johal *et al.*, J. Appl. Phys. **83**, 480 (1998).
[16] C. Goletti *et al.*, J. Appl. Phys. **81**, 3611 (1997).
[17] C. D. MacPherson *et al.*, Phys. Rev. Lett. **77**, 691 (1996).
[18] W. G. Schmidt *et al.*, Phys. Rev. B **57**, 14 596 (1998).

[19] J. Shan, Y. Wang, and R. J. Hamers, J. Phys. Chem. **100**, 4961 (1996).
[20] H. Nienhaus, S. P. Grabowski, and W. Mönch, Surf. Sci. **369**, 196 (1996).
[21] V. M. McConaghie and H. H. Nielsen, J. Chem. Phys. **21**, 1836 (1953).
[22] D. E. Hibbs, C. Jones, and N. A. Smithies, Chem. Commun. (Cambridge) **2**, 185 (1999).
[23] E. R. Nixon, J. Phys. Chem. **60**, 1054 (1955).
[24] Q. Fu, L. Li, C. H. Li, and R. F. Hicks (unpublished).
[25] *Gaussian 98*, Rev. A.6, (Gaussian, Inc., Pittsburgh, 1998).
[26] J. P. Perdew, K. Burke, and Y. Wang, Phys. Rev. B **54**, 16 533 (1996).
[27] N. Godbout *et al.*, Can. J. Chem. **70**, 560 (1992).
[28] G. Igel-Mann, H. Stoll, and H. Preuss, Mol. Phys. **65**, 1321 (1988).
[29] T. H. Dunning, Jr., and P. J. Hay, in *Modern Theoretical Chemistry*, edited by H. F. Schaefer III (Plenum, New York, 1976), Vol. 3, p. 1.
[30] A. Bergner, M. Dolg, W. Kuechle, H. Stoll, and H. Preuss, Mol. Phys. **80**, 1431 (1993).
[31] Q. Fu, L. Li, and R. F. Hicks, Phys. Rev. B (to be published).
[32] Y. J. Chabal, Surf. Sci. Rep. **8**, 211 (1988), and references therein.